MiR-28-3p regulates high glucose-induced endothelial dysfunction by targeting CXXC5

Keywords
peripheral artery disease, high glucose, CXXC5, miR-28-3p, endothelial dysfunction

Abstract

Introduction

Introduction: Data from the CEO database shows microRNA (miR) -28-3p levels are elevated in diabetic patients. Nevertheless, the role of miR-28-3p in peripheral artery disease with diabetes have not been investigated.

Material and methods

The level of miR-28-3p, CXXC5, CXXC-type zinc finger protein 5, and CXXC5's downstream molecules as well as endothelial function were investigated. Dual luciferase analyses were used to confirm the binding site of miR-28-3p and CXXC5.

Results

Results: Under high-glucose condition, miR-28-3p expression is increased whereas CXXC5 expression is downregulated. Overexpression of miR-28-3p increased cell apoptosis and inhibited cell proliferation, migration, and vessel formation, whilst inhibiting its expression had the opposite effect. The overexpression and inhibition of miR-28-3p could also influence both the mRNA and protein levels of CXXC5 and its known downstream molecules. Analysis of bioinformatics data revealed a potential binding site for miR-28-3p and CXXC5. Dual luciferase analyses demonstrated that miR-28-3p suppressed CXXC5 expression by targeting the 3'-untranslated region (3'-UTR) of CXXC5. Following that, we overexpressed both miR-28-3p and CXXC5. The level of CXXC5 and its known downstream signaling molecules decreased with miR-28-3p overexpression alone. As anticipated, co-overexpression of miR-28-3p and CXXC5 partially reversed the effect of miR-28-3p mimics.

Conclusions

Conclusion: These findings indicated that miR-28-3p regulated high glucose-induced endothelial dysfunction by targeting CXXC5.

Abstract

Introduction

Data from the CEO database shows microRNA (miR) -28-3p levels are elevated in diabetic patients. Nevertheless, the role of miR-28-3p in peripheral artery disease with diabetes has not been investigated.

Material and methods

The level of miR-28-3p, CXXC5, CXXC-type zinc finger protein 5, and CXXC5's downstream molecules as well as endothelial function were investigated. Dual luciferase analyses were used to confirm the binding site of miR-28-3p and CXXC5.

Results

Under high-glucose condition, miR-28-3p expression is increased whereas CXXC5 expression is downregulated. Overexpression of miR-28-3p increased cell apoptosis and inhibited cell proliferation, migration, and vessel formation, whilst inhibiting its expression had the opposite effect. The overexpression and inhibition of miR-28-3p could also influence both the mRNA and protein levels of CXXC5 and its known downstream molecules. Analysis of bioinformatics data revealed a potential binding site for miR-28-3p and CXXC5. Dual luciferase analyses demonstrated that miR-28-3p suppressed CXXC5 expression by targeting the 3'-untranslated region (3'-UTR) of CXXC5. Following that, we overexpressed both miR-28-3p and CXXC5. The level of CXXC5 and its known downstream signaling molecules decreased with miR-28-3p overexpression alone. As anticipated, co-overexpression of miR-28-3p and CXXC5 partially reversed the effect of miR-28-3p mimics.

Conclusion

These findings indicated that miR-28-3p regulated high glucose-induced endothelial dysfunction

by targeting CXXC5.

Keywords:

miR-28-3p, high glucose, endothelial dysfunction, peripheral artery disease, CXXC5

Introduction

As life expectancy increases, peripheral artery disease (PAD) is becoming an increasingly severe public health problem. PAD affects roughly 10% of the general population between the ages of 70 and 80 and can reach over 20% at age 80[1, 2]. Clinical studies have shown that diabetes is one of the vital risk factors for PAD[3-5]. In PAD patients with critical limb ischemia, diabetes doubled all-cause mortality[5]. In addition, every 1% increase in HbA1c would lead to a 14.2% increased relative risk for major adverse cardiovascular events[4]. The mechanism by which diabetes worsens PAD prognosis remains unanswered.

MicroRNAs are a class of highly conserved, single-stranded, endogenous non-coding small molecule RNAs, with 20-24 nucleotides in length. They are able to complementarily bind to the 3' non-coding regions (3'UTRs) of their target mRNAs, inhibit the translation of mRNAs, and achieve post-transcriptional regulation, playing an indispensable role in cell development, proliferation, apoptosis as well as differentiation[6]. A few microRNAs, such as miR-21, miR-126, miR-143, and miR-221, have been demonstrated in the regulation of PAD, and provide a therapeutic approach for diagnosis and treatment of diabetes-related complications[7, 8]. miR-28-3p was found to be elevated in type 2 diabetes patients with a 10-year history[9]. In addition, miR-28-3p expression was significantly

higher in type 2 diabetes patients with diabetic retinopathy than in type 2 diabetes patients without diabetic retinopathy[10], indicating that it was associated with the severity of diabetes. In this study, we found that miR-28-3p expression was elevated after analyzing The Gene Expression Omnibus (GEO) data from newly diagnosed type 1 diabetes patients with uncontrolled blood glucose. Its effects on the vascular endothelial remain unknown. In our study, we investigated the function of miR-28-3p in the human umbilical vein endothelial cells (HUVECs). Under high-glucose condition, miR-28-3p expression is increased whereas CXXC5, CXXC-type zinc finger protein 5, expression is downregulated. Overexpression of miR-28-3p increased cell apoptosis and inhibited cell proliferation, migration, and vessel formation. We confirmed miR-28-3p suppressed CXXC5 expression by targeting the 3'-untranslated region (3'-UTR) of CXXC5. CXXC5 functions as a transcriptional regulator by its direct interaction with DNA[11]. It plays a crucial role in the coordination of several signaling pathways, such as transforming growth factor beta (TGF-β), Wnt/β-catenin, ATM/p53[11], and MARK signaling. In addition, it also regulated endothelial cell differentiation and vessel formation in endothelium[12]. As anticipated, co-overexpression of CXXC5 and miR-28-3p partially reversed the endothelium dysfunction caused by the miR-28-3p mimics.

Material and Methods

GEO data Bioinformatics Analysis

Type 1 diabetes gene expression and microRNA expression of 12 samples and 10 control samples were downloaded from the GEO database (GEO accession: GSE55098, GSE55099,https://www.ncbi.nlm.nih.gov/geo/). We used Targetscan (https://www.targetscan.org/vert_80/), Starbase (https://starbase.sysu.edu.cn/), and miRDB

(http://mirdb.org/) to analyze the microRNAs with potential bio-function.

Cell culture

We purchased HUVECs from American Type Culture Collection cell bank. The cells were cultured in DMEM medium and maintained in a humidified atmosphere with 5% CO2 at 37degrees Celsius. To simulate high glucose effects, HUVECs were treated with 33 mM glucose for 24 hours or 48 hours.

Reverse transcription-quantitative PCR (RT-qPCR)

We extracted total RNA from HUVECs using the Trizol Reagent (Aidlab Biotechnologies Co., Ltd) according to the manufacturer's protocol. Total RNA was then reversely transcribed into cDNA using Hiscript Reverse transcriptase (Nanjing Vazyme Biotech Co., Ltd.). We used U6 and GAPDH as the internal control for microRNA and proteins, respectively. The RT-qPCR reaction was conducted using the SYBR Green Master Mix (Nanjing Vazyme Biotech Co., Ltd.) at 50degrees Celsius for two minutes, 95degrees Celsius for ten minutes, followed by 40 cycles of 95degrees Celsius for thirty seconds, and 60degrees Celsius for thirty seconds. We calculated the relative expression of each mRNA or miRNA using the 2-ΔΔCt method. The experiments were performed via QuantStudio6 (Applied Biosystems, Inc.). All the primers used are listed as follows: GAPDH Forward 5'-TCAAGAAGGTGGTGAAGCAGG -3', Reverse 5'-TCAAAGGTGGAGGAGTGGGT -3'. CXXC5 Forward 5'- CCGCTCTCCCACTACTCTTC -3', Reverse 5'- GAGGTAGGGTTGCTTTTGTCC -3'. Flk-1 Forward TACGTTGGAGCAATCCCTGT, Reverse TACACTTTCGCGATGCCAAG. TGF - β Forward CAGCAACAATTCCTGGCGATACCT, Reverse CGCTAAGGCGAAAGCCCTCAAT. U6 Forward 5'- CGCTTCGGCAGCACATATAC -3', Reverse 5'- AAATATGGAACGCTTCACGA -3'. miR-28-3p F primer TGCGCCACTAGATTGTGAGCTC, loop primer

GTCGTATCCAGTGCAGGGTCCGAGGTATTCGCACTGGATACGACTCCAGGAG. mircoRNA universal antisense primer, R primer: CCAGTGCAGGGTCCGAGGTATT.

Plasmid Construction

To overexpress the CXXC5 gene, the FV144-ZsGreen-CON plasmid was used to construct CXXC5 overexpression vectors. The CXXC5 gene was obtained and amplified from hCXXC5-OE plasmid. We used the Seamless Cloning technique to insert the CXXC5 gene into the FV144-ZsGreen-CON plasmid. All fragments generated through PCR amplification and recombinant plasmid were sequenced to validate mutations in each fragment.

Cell transfection

After seeding HUVECs into a 6-well plate at a density of 1x10E5 cells per well, cells were cultured until they reached a confluence of 50-60%. Then, transfection of microRNAs and plasmids into HUVECs was performed using Lipofectamine® 2000 (Invitrogen; Thermo Fisher Scientific, Inc.) following the manufacturer's protocol. Briefly, 5 μl of Lipofectamine 2000 was added to 200 μl of serum-free RPMI-1640 medium and incubated for 5 minutes at room temperature. Subsequently, an appropriate amount of miR-28-3p mimic, miR-28-3p inhibitor, negative control, or pcDNA was added to the Lipofectamine mixture and incubated for an additional 20 minutes at room temperature. The final transfection mixture was then added to each well and incubated with the cells at 37degrees Celsius for 24 hours. For the high glucose group, HUVECs were treated with 33 mM glucose for 24 or 48 hours for the subsequent experiments.

Cell proliferation

HUVECs were firstly seeded into 96-well plates at 3x10E3 cells/well, and then cultured for 24 hours and received transfection of microRNA or plasmid for 6 hours. After removing the transfection

buffer, the cells were incubated in a normal medium for another 24 hours and received high glucose treatment for 48 hours in the high glucose group. Following the incubation, 10 μl Cell Counting Kit-8 solution (CCK-8 kit, Elabscience Biotechnology Co., Ltd) was added to each well and we incubated it for another 4 hours at 37 degrees Celsius. In the end, we measured the absorbance at a wavelength of 450 nm.

Cell migration

We used Transwell assays to detect the migration of HUVECs. HUVECs were suspended at a concentration of 4x10E5 cells/ml in serum-free RPMI1640 media. 800ul of 10% fetal bovine serum was added to each well on a 24-well plate. Then 200ul of HUVECs were loaded in each Transwell plate (Corning, Inc.) and placed in the well. We used a cotton swab to remove cells that remained in the upper chamber after 24 hours of incubation and fixed the cells that had migrated to the lower chamber with 70% iced ethanol for 1 hour at room temperature. Then we stained cells in the lower chamber with 0.5% crystal violet for 20 minutes at room temperature. Using a light microscope, we observed migratory cells from each group and counted their numbers in three randomly chosen fields of view (magnification, x200; Olympus Corporation).

Apoptosis analysis by flow cytometry

We detected cell apoptosis using an AnnexinV-FITC/PI kit (Elabscience Biotechnology Co., Ltd) according to the manufacturer's instructions. Following transfection, cell collection, and preparation, the HUVECs were stained for 15 minutes in the dark at room temperature with 5 ml Annexin V and 5 ml PI. Using a BD FACSVerseTM flow cytometer (BD Biosciences Co., Ltd), apoptotic cells were studied and we analyzed the data using FlowJo software Version 10.4. (FlowJo Co., Ltd).

Vessel formation assay

We dissolved The Matrigel (Corning) and put 24‐well plates at four degrees overnight. Then, we added 100 μL Matrigel to the 24‐well plate, which was then centrifuged to remove bubbles. After centrifugation, we put the plates at 37 degrees Celsius for 1 hour with 1 × 10E5 HUVECs added into each well. Following that, the cells were incubated for another 12 hours and visualized by microscope. Vessel formation from each well was observed and counted in three randomly chosen fields of view (magnification, x100; Olympus Corporation) and analyzed by ImageJ software.

Protein extraction and Western blotting

We washed HUVECs at least twice with cold PBS buffer. Then, we added RIPA lysis buffer (Beyotime Institute of Biotechnology) supplemented with phenylmethanesulfonyl fluoride (Beyotime) and sodium orthovanadate (Beyotime) into each well, followed by a 30-minute incubation period on ice. Following lysis, cells were carefully scraped from one side of the cell plate and the resulting mixture of cell debris and the lysate was collected into a 1.5ml centrifuge tube and centrifuged at 12000rpm for 5 minutes at 4 degrees Celsius. The supernatant was then collected and transferred to a 0.5ml centrifuge tube. The total protein concentration was measured using the BCA method. Protein samples were subjected to SDS‐PAGE (40 ug proteins were loaded in each well) and then transferred to the PVDF membrane. Primary antibodies, including GAPDH （1:1000 Affinity）, P65 (1:1000 Boster), p-p65 (1:1000 Affinity), TGF-B (1:1000 Abcam), P38 (1:1000 Bioss) and p-p38 (1:1000 Affinity), were incubated with the membrane overnight. Then we incubated the membranes with secondary antibodies (1:5000) at room temperature for another 2 hours and used the enhanced chemiluminescence method to analyze the results.

Vector construction and dual-Luciferase activity assay

We used TargetScan (www.targetscan.org) to predict that CXXC5 (3' UTR)was the binding site of

miR-28-3p. We used a pYr-MirTarget miRNA target expression vector to contain a wild-type (WT) or mutant (Mut) CXXC5 untranslated region (3'UTR). 293T cells were seeded in 12-well plates (1x10E5 cells/well) to obtain a cell confluence of 50-60%. The microRNAs and plasmid were co-transfected into 293T cells via Lipofectamine® 2000 (Invitrogen; Ther mo Fisher Scientific, Inc.). After 48 hours of incubation, luciferase activity was assessed through a dual luciferase reporter assay (Beyotime Biotechnology). We normalized firefly luciferase activity to Renilla luciferase activity.

Statistical analysis

We presented Data as mean ± SD and used two-tailed Student's t-test to compare continuous data. Statistical analysis was performed via GraphPad Prism software version 5.0 (GraphPad Software, Inc.). P-value < .05 was considered statistically significant.

Results

1. miR-28-3p and CXXC5 expression in high-glucose conditions

Expression profiling including microRNAs and proteins was obtained from Gene Expression Omnibus (GSE55098, GSE 55099). A total of 12 newly diagnosed diabetes Type 1 patients and 10 normal controls were collected and analyzed. Their demographic characteristics were provided in Supplementary Table 1. The two Gene Expression Omnibus showed that the miR-28-3p level (Fig. 1A) was up-regulated and the CXXC5 level (Fig. 1B) was down-regulated (indicating a trend, though not reaching statistical difference). To further confirm these results, we subjected HUVECs to high glucose conditions (33mM glucose for 24 hours and 48 hours, respectively) to simulate diabetes. The results from HUVECs were consistent with GEO data, showing the increase in miR-28-3p level and decrease in CXXC5 level after exposure to high glucose impact (Fig. 1C & D).

2. miR-28-3p was related to high-glucose-induced endothelial dysfunction and regulated CXXC5 expression

We studied the effect of miR-28-3p on HUVECs. After transfection of HUVECs with miR-28-3p mimics as well as inhibitors, miR-28-3p level was significantly upregulated and downregulated, respectively (Fig. 2A). The effects of miR-28-3p on cell migration and death were then investigated via CCK8 and flow cytometry. CCK8 analysis revealed that transfection with miR-28-3p mimics under normal conditions could impair cell proliferation while transfection with miR-28-3p inhibitors under high glucose would reverse the cell proliferation (Fig. 2D). Flow cytometry showed that miR-28-3p mimics increased the apoptosis of HUVECs under normal condition while miR-28-3p inhibitors decreased the apoptosis under high glucose. (Fig. 2C and Supplementary fig. 1). We also assessed the CXXC5 level and its known downstream signaling molecules, Flk-1 (a receptor for vascular endothelial growth factor, also named as vascular endothelial growth factor receptor 2) and TGF-β (transforming growth factor beta, a multifunctional cytokine regulating cell growth and differentiation). PCR results showed that CXXC5 was decreased with miR-28-3p mimics and increased with miR-28-3p inhibitors (Fig. 2B), along with the synchronized expression of both Flk-1 (Fig. 2E) and TGF-β (Fig. 2F).

We also detected the role of miR-28-3p on migration and vessel formation. Transwell assays and vessel formation assays showed that HUVECs' abilities on migratory and vessel formation were significantly decreased under miR-28-3p overexpression compared with those in the NC group (Fig. 2G & 2H, Fig. 2L & 2M). On the other hand, the migration and vessel formation was significantly elevated in the miR-28-3p inhibitor group compared with those in the inhibitor NC group (Fig. 2I & 2J, Fig. 2N & 2O). Fig. 2K and Fig. 2P & 2Q showed quantitative results of migration and vessel

formation, respectively. These results suggested that miR-28-3p played a negative role in high glucose-induced endothelial dysfunction. In addition, we detected the effects of miR-28-3p on CXXC5 and its known downstream signaling molecules, TGF-β, P38, and P65, through Western blot. Similar expression patterns for CXXC5 were discovered by Western blot and PCR (Fig. 2R). CXXC5's known downstream signaling molecules exhibited synchronized expression patterns (Fig. 2S).

3. CXXC5 serves as a direct target gene of miR-28-3p

We used miRDB (http://mirdb.org/), Targetscan (https://www.targetscan.org/vert_80/), and Starbase (https://starbase.sysu.edu.cn/) to predict the possible gene target of miR-28-3p. The 3'-UTR of CXXC5 was predicted to have a complementary binding site for the seed region of miR-28-3p. (Fig. 3A-B). To further test if miR-28-3p targeted CXXC5, we used a dual luciferase reporter assay to determine their relationship in the 293T cell line. As shown in Fig. 3C, transfection with the miR-28-3p mimic led to a significant reduction in terms of the luciferase activity of the CXXC5-WT 3'-UTR compared with those transfected with mimic NC. The effect disappeared when the binding site of the CXXC5 3'-UTR was mutated, which suggested that CXXC5 may be a direct target gene of miR-28-3p.

4. Effect of miR-28-3p mimics and CXXC5 overexpression in HUVECs

To further understand the mechanism on miR-28-3p and CXXC5 affecting the HUVECs function, the effect of their overexpression on HUVECs function and CXXC5 downstream molecules was investigated. As illustrated in Fig. 4, these results indicated that transfection with the miR-28-3p mimics significantly increased apoptosis (also refer to Supplementary Fig. 2) and decreased cell proliferation. The level of CXXC5 and its downstream molecules, Flk-1 and TGF-β, were decreased. Intriguingly, the co-overexpression of CXXC5 partially reversed the effects of the miR-28-3p mimic on endothelial dysfunction and its downstream molecules.

We also detected the effect of co-overexpression of both miR-28-3p and CXXC5 on migration and vessel formation. Transwell assays (Fig. 4G-4J) and vessel formation assays (Fig. 4K-4O) revealed that the migratory and vessel formation abilities of HUVECs were significantly reduced in the miR-28-3p mimic group and can be partially reversed when CXXC5 was overexpressed at the same time. In addition, we detected the effects of co-overexpression of both miR-28-3p and CXXC5 and its known downstream signaling molecules, TGF-β, P38, and P65, through Western blot. As anticipated, the level of CXXC5 and its downstream signaling molecules, TGF-β, phosphorylated P38, and phosphorylated P65, was decreased with miR-28-3p mimics and the overexpression of CXXC5 partially reversed the effect of miR-28-3p mimics (Fig. 4P-4R).

Discussion

PAD is characterized by narrowed arteries reducing blood flow to the lower extremities and gets complicated when the patients have comorbidities such as diabetes and hypertension[4, 13]. Several microRNAs, including miR-142, miR-221, miR-143, miR-21, and miR-210, have been identified in the natural progression of PAD[14-16]. Targeting the microRNAs in exosomes may be a viable therapeutic technique for the treatment of cardiovascular complications associated with diabetes[7]. In addition, there are trials using locked nucleic acid-modified microRNA to inhibit the corresponding microRNA that was overexpressed in disease states[17]. miR-28-3p was discovered to have a biological function role in several diseases. The level of circulating miR-28-3p has significantly changed in several diseases, including severe asthma[18], colorectal cancer[19], gastric cancer[20], amyotrophic lateral sclerosis[21], non-ST-segment elevation acute coronary syndrome[22], pulmonary embolism[23], prostate cancer[24], diabetes with coronary heart disease[25] as well as diabetes retinopathy[10], and can be a marker for detecting these diseases. Previous studies also showed that miR-28-3p could inhibit

prostate cancer cell proliferation and migration as well as invasion, promotes apoptosis by targeting ARF6 [26], and regulated myogenic differentiation and inhibition of rhabdomyosarcoma progression[27]. It also played a role in cell migration and invasion in nasopharyngeal cancer cells[28] and non-small cell lung cancer cells [29]. Nevertheless, there were no reports on the role of miR-28-3p in PAD with diabetes.

In the present study, we used data from the GEO database to analyze the microRNAs with potential bio-function. The expression of miR-28-3p was found to be upregulated while the CXXC5 was downregulated in diabetic patients compared with healthy controls in both GEO databases and further verified in HUVECs. Therefore, we hypothesized that miR-28-3p might play a role in endothelial function with high glucose. To confirm this hypothesis, we used HUVECs with high glucose to simulate PAD with diabetes. We discovered that miR-28-3p overexpression would induce cell apoptosis, and inhibit cell proliferation and migration as well as vessel formation, while the inhibition of its expression showed the opposite function. The overexpression and inhibition of miR-28-3p could also regulate the CXXC5 level and its known downstream molecules on both the mRNA level and protein level. In addition, bioinformatics analysis showed a possible binding site for the miR-28-3p and CXXC5. These data indicated that CXXC5 may be involved in miR-28-3p-mediated HUVECs function.

As one member of the CXXC-type zinc-finger protein family, CXXC5 is able to act as a transcriptional regulator by directly binding to DNA[11]. CXXC5 gene expression is regulated by a number of cytokines, intracellular transcription factors as well as microRNAs[30]. In addition, CXXC5 itself played an important role in coordinating various signaling pathways, including those initiated by TGF-β, bone and morphogenetic proteins, Wnt/β-catenin, ATM/p53[11], and MARK signaling (Erk 1/2,

p38, and c-Jun N-terminal kinase)[31]. CXXC5 is related to cell apoptosis in hepatocellular carcinoma[32], esophageal squamous cell carcinoma[30], and gastric cancer[33], and downregulation of CXXC5 is associated with a better prognosis in acute myeloid leukemia[34]. Additionally, CXXC5 is able to negatively regulate cutaneous wound healing[35]. In terms of endothelial function, it is reported to be a transcriptional activator of Flk-1, regulating endothelial cell differentiation and vessel formation[12].

In the current study, the luciferase assay indicated that miR-28-3p inhibited the expression levels of CXXC5 by targeting 3′-UTR of CXXC5. And we overexpressed both miR-28-3p and CXXC5. As expected, the level of CXXC5 and its known downstream signaling molecules was decreased with miR-28-3p mimics alone while the overexpression of CXXC5 at the same time partially reverse the effect of miR-28-3p mimics.

Conclusions

In conclusion, our study provided experimental in vitro evidence, indicating that miR-28-3p inhibits vascular endothelial function by targeting CXXC5 in high-glucose cultured HUVECs. The limitation is the lack of in vivo experiments. There is still a long way ahead to translate the basic medical research of miR-28-3p into clinical application. The mechanisms revealed by our results imply that miR-28-3p may serve as a promising target in the treatment of PAD with diabetes.

Declarations

Ethics approval and consent to participate: The authors are accountable for all aspects of the work in ensuring that questions related to the accuracy or integrity of any part of the work are appropriately investigated and resolved. Experiments were performed under a project license granted by the

Institutional Review Board of the Ethics Committee of Zhejiang University, in compliance with Chinese guidelines for the care and use of animals.

Consent for publication: Not applicable

Availability of data and materials: The datasets used and/or analyzed during the current study are available from the corresponding author on reasonable request.

Competing interests: The authors declare that they have no competing interests.

Funding: This study was supported by the Health Commission of Zhejiang Province (Grant No. 2021KY904) and the National Natural Science Foundation of China (Grant No. 81970694).

Author Contributions: Conceptualization, LW and CQ; Data curation, LW, JP, and CQ; Formal analysis, XF and YD; Funding acquisition, ZW and CQ; Investigation, LW, YD and CQ; Methodology, SW, ZW, and CQ; Resources, XF, SW and ZW; Supervision, ZW and XF; Writing – original draft, CQ and JP; Writing – review & editing, LW, CQ, and ZW. All authors have read and agreed to the published version of the manuscript.

Acknowledgments: Not applicable

Reference

1. Fowkes, F.G., V. Aboyans, F.J. Fowkes, et al., *Peripheral artery disease: epidemiology and global perspectives.* Nat Rev Cardiol, 2017. **14**(3): p. 156-170.
2. Song, P., D. Rudan, Y. Zhu, et al., *Global, regional, and national prevalence and risk factors for peripheral artery disease in 2015: an updated systematic review and analysis.* Lancet Glob Health, 2019. **7**(8): p. e1020-e1030.
3. Cai, M., Y. Xie, B. Bowe, et al., *Temporal Trends in Incidence Rates of Lower Extremity Amputation and Associated Risk Factors Among Patients Using Veterans Health Administration Services From 2008 to 2018.* JAMA Netw Open, 2021. **4**(1): p. e2033953.
4. Low Wang, C.C., J.I. Blomster, G. Heizer, et al., *Cardiovascular and Limb Outcomes in Patients With Diabetes and Peripheral Artery Disease: The EUCLID Trial.* J Am Coll Cardiol, 2018. **72**(25): p. 3274-3284.

5. Vrsalovic, M., K. Vucur, A. Vrsalovic Presecki, et al., *Impact of diabetes on mortality in peripheral artery disease: a meta-analysis.* Clin Cardiol, 2017. **40**(5): p. 287-291.
6. Van Meter, E.N., J.A. Onyango, and K.A. Teske, *A review of currently identified small molecule modulators of microRNA function.* Eur J Med Chem, 2020. **188**: p. 112008.
7. Zhao, S., H. Wang, H. Xu, et al., *Targeting the microRNAs in exosome: A potential therapeutic strategy for alleviation of diabetes-related cardiovascular complication.* Pharmacol Res, 2021. **173**: p. 105868.
8. Kumar, S., D. Williams, S. Sur, et al., *Role of flow-sensitive microRNAs and long noncoding RNAs in vascular dysfunction and atherosclerosis.* Vascul Pharmacol, 2019. **114**: p. 76-92.
9. Zampetaki, A., S. Kiechl, I. Drozdov, et al., *Plasma microRNA profiling reveals loss of endothelial miR-126 and other microRNAs in type 2 diabetes.* Circ Res, 2010. **107**(6): p. 810-7.
10. Liang, Z., K.P. Gao, Y.X. Wang, et al., *RNA sequencing identified specific circulating miRNA biomarkers for early detection of diabetes retinopathy.* Am J Physiol Endocrinol Metab, 2018. **315**(3): p. E374-e385.
11. Xiong, X., S. Tu, J. Wang, et al., *CXXC5: A novel regulator and coordinator of TGF-β, BMP and Wnt signaling.* J Cell Mol Med, 2019. **23**(2): p. 740-749.
12. Kim, H.Y., D.H. Yang, S.W. Shin, et al., *CXXC5 is a transcriptional activator of Flk-1 and mediates bone morphogenic protein-induced endothelial cell differentiation and vessel formation.* Faseb j, 2014. **28**(2): p. 615-26.
13. Golledge, J., *Update on the pathophysiology and medical treatment of peripheral artery disease.* Nat Rev Cardiol, 2022. **19**(7): p. 456-474.
14. Ismaeel, A., E. Fletcher, D. Miserlis, et al., *Skeletal muscle MiR-210 expression is associated with mitochondrial function in peripheral artery disease patients.* Transl Res, 2022. **246**: p. 66-77.
15. Barbalata, T., O.E. Moraru, C.S. Stancu, et al., *Increased miR-142 Levels in Plasma and Atherosclerotic Plaques from Peripheral Artery Disease Patients with Post-Surgery Cardiovascular Events.* Int J Mol Sci, 2020. **21**(24).
16. Sorrentino, T.A., P. Duong, L. Bouchareychas, et al., *Circulating exosomes from patients with peripheral artery disease influence vascular cell migration and contain distinct microRNA cargo.* JVS Vasc Sci, 2020. **1**: p. 28-41.
17. Gallant-Behm, C.L., J. Piper, B.A. Dickinson, et al., *A synthetic microRNA-92a inhibitor (MRG-110) accelerates angiogenesis and wound healing in diabetic and nondiabetic wounds.* Wound Repair Regen, 2018. **26**(4): p. 311-323.
18. Kyyaly, M.A., T. Sanchez-Elsner, P. He, et al., *Circulating miRNAs-A potential tool to identify severe asthma risk?* Clin Transl Allergy, 2021. **11**(4): p. e12040.
19. Silva, C.M.S., M.C. Barros-Filho, D.V.T. Wong, et al., *Circulating let-7e-5p, miR-106a-5p, miR-28-3p, and miR-542-5p as a Promising microRNA Signature for the Detection of Colorectal Cancer.* Cancers (Basel), 2021. **13**(7).
20. Guo, Y., X. Cui, Y. Zhang, et al., *Diagnostic and Prognostic Value of Serum miR-296-5p and miR-28-3p in Human Gastric Cancer.* Cancer Biother Radiopharm,

2020.
21. Liguori, M., N. Nuzziello, A. Introna, et al., *Dysregulation of MicroRNAs and Target Genes Networks in Peripheral Blood of Patients With Sporadic Amyotrophic Lateral Sclerosis.* Front Mol Neurosci, 2018. **11**: p. 288.
22. Wang, A., L.C. Kwee, E. Grass, et al., *Whole blood sequencing reveals circulating microRNA associations with high-risk traits in non-ST-segment elevation acute coronary syndrome.* Atherosclerosis, 2017. **261**: p. 19-25.
23. Zhou, X., W. Wen, X. Shan, et al., *MiR-28-3p as a potential plasma marker in diagnosis of pulmonary embolism.* Thromb Res, 2016. **138**: p. 91-95.
24. McDonald, A.C., M. Vira, V. Walter, et al., *Circulating microRNAs in plasma among men with low-grade and high-grade prostate cancer at prostate biopsy.* Prostate, 2019. **79**(9): p. 961-968.
25. Jiménez-Lucena, R., O.A. Rangel-Zúñiga, J.F. Alcalá-Díaz, et al., *Circulating miRNAs as Predictive Biomarkers of Type 2 Diabetes Mellitus Development in Coronary Heart Disease Patients from the CORDIOPREV Study.* Mol Ther Nucleic Acids, 2018. **12**: p. 146-157.
26. Zhang, J., Y. Yao, H. Li, et al., *miR-28-3p inhibits prostate cancer cell proliferation, migration and invasion, and promotes apoptosis by targeting ARF6.* Exp Ther Med, 2021. **22**(5): p. 1205.
27. Skrzypek, K., A. Nieszporek, B. Badyra, et al., *Enhancement of myogenic differentiation and inhibition of rhabdomyosarcoma progression by miR-28-3p and miR-193a-5p regulated by SNAIL.* Mol Ther Nucleic Acids, 2021. **24**: p. 888-904.
28. Lv, Y., H. Yang, X. Ma, et al., *Strand-specific miR-28-3p and miR-28-5p have differential effects on nasopharyngeal cancer cells proliferation, apoptosis, migration and invasion.* Cancer Cell Int, 2019. **19**: p. 187.
29. Zhou, X., Y. Feng, S. Liu, et al., *IL-33 Promotes the Growth of Non-Small Cell Lung Cancer Cells Through Regulating miR-128-3p/CDIP1 Signalling Pathway.* Cancer Manag Res, 2021. **13**: p. 2379-2388.
30. Liu, Y.T., D. Zong, X.S. Jiang, et al., *miR-32 promotes esophageal squamous cell carcinoma metastasis by targeting CXXC5.* J Cell Biochem, 2019. **120**(4): p. 6250-6263.
31. Ma, L., X. Wang, H. Liu, et al., *CXXC5 Mediates P. gingivalis-suppressed Cementoblast Functions Partially via MAPK Signaling Network.* Int J Biol Sci, 2019. **15**(8): p. 1685-1695.
32. Yan, X., J. Wu, Q. Jiang, et al., *CXXC5 suppresses hepatocellular carcinoma by promoting TGF-β-induced cell cycle arrest and apoptosis.* J Mol Cell Biol, 2018. **10**(1): p. 48-59.
33. Chen, X., X. Wang, L. Yi, et al., *The KN Motif and Ankyrin Repeat Domains 1/CXXC Finger Protein 5 Axis Regulates Epithelial-Mesenchymal Transformation, Metastasis and Apoptosis of Gastric Cancer via Wnt Signaling.* Onco Targets Ther, 2020. **13**: p. 7343-7352.
34. Kühnl, A., P.J. Valk, M.A. Sanders, et al., *Downregulation of the Wnt inhibitor CXXC5 predicts a better prognosis in acute myeloid leukemia.* Blood, 2015. **125**(19): p. 2985-94.

35. Lee, S.H., M.Y. Kim, H.Y. Kim, et al., *The Dishevelled-binding protein CXXC5 negatively regulates cutaneous wound healing.* J Exp Med, 2015. **212**(7): p. 1061-80.

Figure legend

Fig. 1 miR-28-3p and CXXC5 expression. the miR-28-3p level increased and the CXXC5 level decreased under high glucose conditions. The CXXC5 level in 1B indicated a decreasing trend among diabetic patients, though did not reach statistical significance. 12 diabetes patients vs 10 normal controls. 1A, 1B: from Gene Expression Omnibus (GSE55098, GSE 55099). 1C, 1D: HUVECs in normal glucose and high glucose. *P < 0.05, **P < 0.01, ***P < 0.001.

Fig. 2 Molecular expression and HUVEC function under miR-28-3p mimics and inhibitors. 2A, 2B, 2E, and 2F: PCR results; 2C: Apoptosis detected by flow cytometry; 2D. Cell proliferation assessed by CCK8. Fig 2G-2K: Cell migration detected by Transwell assays. Fig. G: Control+NC; Fig. H: Control+miR-28 mimics; Fig. I: HG+NC; Fig. J: HG+miR-28 inhibitor. Fig. G to J: one representative picture of Transwell assays. Fig. K: quantitative analysis of Transwell assays. Fig L-Q: Vessel formation assay. L: Control+NC; Fig. M: Control+miR-28 mimics; Fig. N: HG+NC; Fig. O: HG+miR-28 inhibitor. Fig. L to O: one representative picture of vessel formation assay. Fig. P & Q: quantitative analysis of vessel formation. Fig R and S: Western blot results on CXXC5 and its known downstream signaling molecules. GAPDH is the internal reference. P-P65: Phosphorylated P65; P-P38: Phosphorylated P38. Control+NC: HUVECs in normal glucose level with negative control; Control+miR-28 mimics: HUVECs in normal glucose level with miR-28-3p mimics (1uM for 48 hours); HG+NC: HUVECs under high glucose for 48 hours with negative control; HG+miR-28

inhibitor, HUVECs under high glucose for 48 hours with miR-28-3p inhibitors for 48 hours. *P < 0.05, **P < 0.01, ***P < 0.001.

Fig. 3 CXXC5 is a direct target gene of miR-28-3p. Fig 3A: We used Targetscan, Starbase, and miRDB to predict the possible gene target of miR-28-3p in GSE55098, a dataset consisting of proteins from newly diagnosed type 1 diabetic patients. Only two proteins, namely CXXC5 and PARP8, poly(ADP-Ribose) polymerase family member 8, were found to be the potential target. There was no observed correlation between the expression levels of PARP8 and miR-28-3p in high-glucose cultured HUVEC. Therefore, the subsequent investigations were centered on miR-28-3p and CXXC5. Fig. 3B, prediction of miR-28-3p binding sites in the 3'-UTR of the CXXC5 gene, along with the mutated 3' UTR for dual luciferase reporter assay. Fig. 3C, dual luciferase reporter assay. Transfection with the miR-28-3p mimic significantly decreased the relative luciferase activity of the CXXC5-WT 3'-UTR compared with that in cells following the transfection of mimic NC. The effect was abolished when the nucleotides in the seed binding site of the CXXC5 3'-UTR were mutated. *P < 0.05, **P < 0.01, ***P < 0.001.

Fig. 4 Molecular expression and HUVECs function under miR-28-3p mimics and CXXC5 overexpression. 4A, 4B, 4E, 4F: PCR results; C: Apoptosis detected by flow cytometry; 4D. Cell proliferation assessed by CCK8. 4A, 4B, 4E, 4F: PCR results; 4C: Apoptosis detected by flow cytometry; 4D. Cell proliferation assessed by CCK8. Fig 4G-4J: Cell migration detected by Transwell assays. Cell migration detected by Transwell assays. Fig. 4G: Negative control; Fig. 4H: miR-28 mimics; Fig. 4I: miR-28 mimics+CXXC5 plasmid. Fig. 4G to I: one representative picture of vessel

formation assay. Fig. 4J: quantitative analysis of Transwell assays. Fig 4K-4O: Vessel formation assay. Fig. 4K: Negative control; Fig. 4L: miR-28 mimics; Fig. 4M: miR-28 mimics+CXXC5 plasmid. Fig. 4K to 4M: one representative picture of vessel formation assay. Fig. 4N & 4O: quantitative analysis of vessel formation. Fig 4P-4R: Western blot results on co-overexpression of both miR-28-3p and CXXC5. GAPDH is the internal reference. P-P65: Phosphorylated P65; P-P38: Phosphorylated P38. Negative control: HUVECs in normal glucose level with negative control; miR-28 mimics: HUVECs in normal glucose level with miR-28-3p mimics (1uM for 48 hours); miR-28 mimics+CXXC5 plasmid: HUVECs in normal glucose level with miR-28-3p mimics and CXXC5 overexpression plasmid. *P < 0.05, **P < 0.01, ***P < 0.001.

Fig. 5 Diagram of the role of miR-28 in high glucose-cultured HUVEC

Supplementary Fig. 1 Typical flow cytometry results in apoptosis of Fig 2C. Control+NC: HUVECs in normal glucose level with negative control; Control+miR-28 mimics: HUVECs in normal glucose level with miR-28-3p mimics; HG+NC: HUVECs under high glucose for 48 hours with negative control; HG+miR-28 inhibitor, HUVECs under high glucose for 48 hours with miR-28-3p inhibitors for 48 hours.

Supplementary Fig. 2 Typical flow cytometry results in apoptosis of Fig 4C. Control: HUVECs in normal glucose level with negative control; miR-28 mimics: HUVECs in normal glucose level with miR-28-3p mimics (1uM for 48 hours); miR-28 mimics+CXXC5 plasmid: HUVECs in normal glucose level with miR-28-3p mimics and CXXC5 overexpression plasmid.

Graphical Abstract Under high-glucose condition, miR-28-3p expression is increased in the human umbilical vein endothelial cells (HUVECs). miR-28-3p suppressed CXXC5 expression by targeting the 3'-untranslated region (3'-UTR) of CXXC5. CXXC5, CXXC-type zinc finger protein 5, functions as a transcriptional regulator and is essential for the coordination of various signaling pathways, including Flk-1, transforming growth factor beta (TGF-β) signaling pathway, MARK signaling pathway. The downregulation of CXXC5 is observed when miR-28-3p is overexpressed. Consequently, this downregulation leads to a decrease in the proliferation, migration, and vessel formation capabilities of HUVECs, and an increase in the apoptosis.

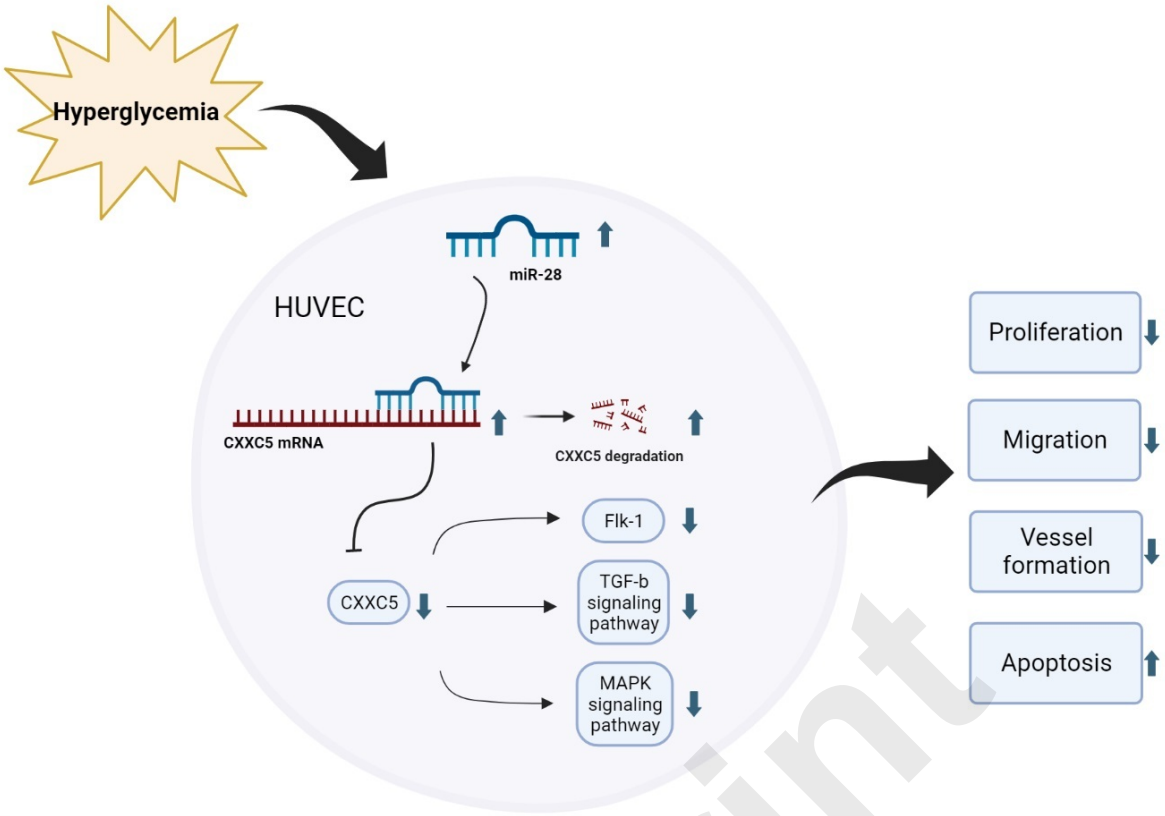
Hyperglycemia
HUVEC
miR-28
CXXC5 mRNA
CXXC5 degradation
Flk-1
CXXC5
TGF-b signaling pathway
MAPK signaling pathway
Proliferation
Migration
Vessel formation
Apoptosis

Supplementary Table 1: demographic characteristics of patients in GEO accessions: GSE55098, GSE55099

	Control (n = 10)	Type 1 diabetes (n = 12)
No. women/men	6/4	5/7
Age (years)	18.70 ± 1.16	17.50 ± 3.68
FBG (mmol/L)	4.78 ± 0.20	6.37 ± 1.93*
HbA1c (%)	5.29 ± 0.42	11.78 ± 3.63***
GADA (U/mL)	2.50 (1.87–2.91)	149.85 (47.30–319.33)**
Fasting C peptide (ng/mL)	2.08 ± 0.77	0.47 ± 0.20***

FBG, fasting blood glucose; GADA, glutamic acid decarboxylase antibody. Values are given as the mean ± SD or as median values with the interquartile range in parentheses. *P < 0.05, **P < 0.01, ***P < 0.0001 compared with normal

Data are obtained from Decreased miR-146 expression in peripheral blood mononuclear cells is correlated with ongoing islet autoimmunity in type 1 diabetes patients 1miR-146. J Diabetes 2015 Mar;7(2):158-65.

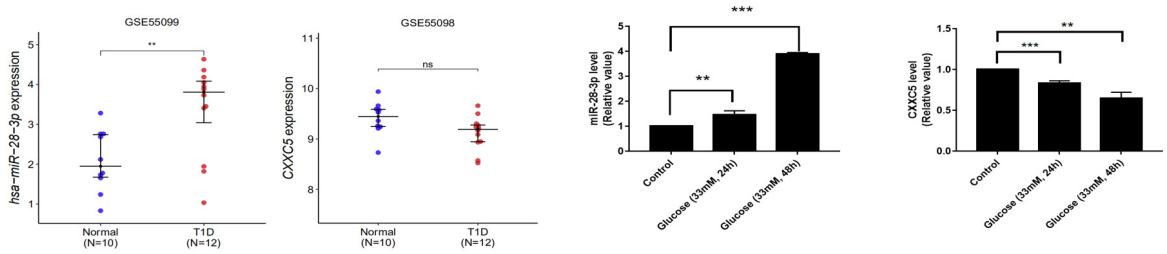

1A 1B 1C 1D

miR-28-3p and CXXC5 expression. the miR-28-3p level increased and the CXXC5 level decreased under high glucose conditions. The CXXC5 level in 1B indicated a decreasing trend among diabetic patients, though did not reach statistical significance. 12 diabetes patients vs 10 normal controls. 1A, 1B: from Gene Expression Omnibus (GSE55098, GSE 55099). 1C, 1D: HUVECs in normal glucose and high glucose. *P < 0.05, **P < 0.01, ***P < 0.001.

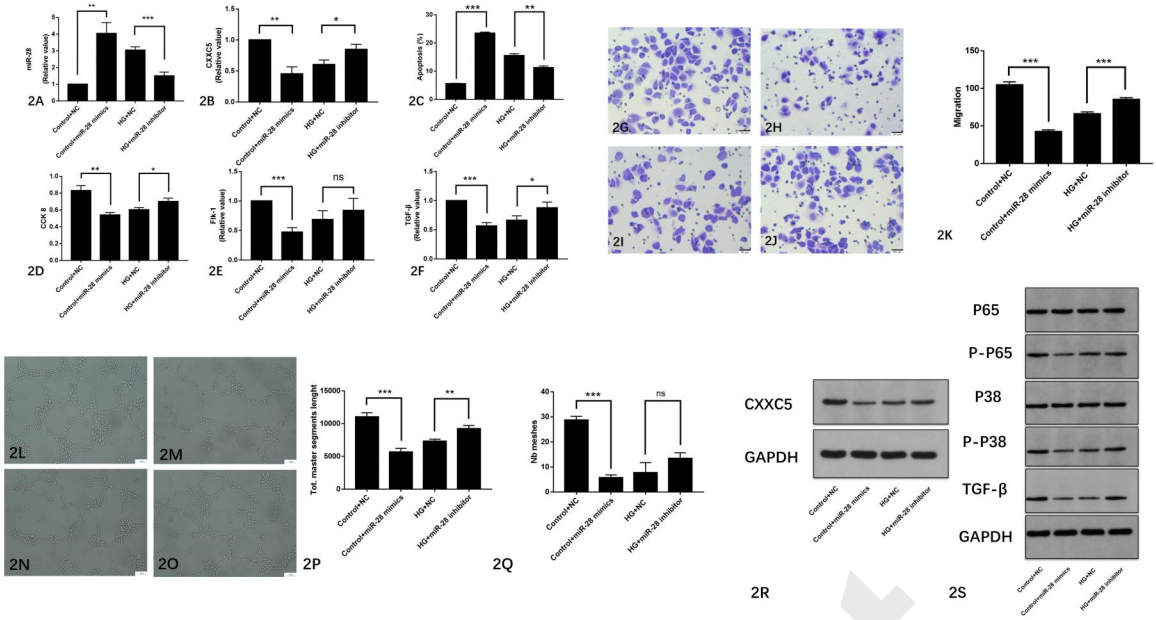

Molecular expression and HUVEC function under miR-28-3p mimics and inhibitors. 2A, 2B, 2E, and 2F: PCR results; 2C: Apoptosis detected by flow cytometry; 2D. Cell proliferation assessed by CCK8. Fig 2G-2K: Cell migration detected by Transwell assays. Fig. G: Control+NC; Fig. H: Control+miR-28 mimics; Fig. I: HG+NC; Fig. J: HG+miR-28 inhibitor. Fig. G to J: one representative picture of Transwell assays. Fig. K: quantitative analysis of Transwell assays. Fig L-Q: Vessel formation assay. L: Control+NC; Fig. M: Control+miR-28 mimics; Fig. N: HG+NC; Fig. O: HG+miR-28 inhibitor. Fig. L to O: one representative picture of vessel formation assay. Fig. P & Q: quantitative analysis of vessel formation. Fig R and S: Western blot results on CXXC5 and its known downstream signaling molecules. GAPDH is the internal reference. P-P65: Phosphorylated P65; P-P38: Phosphorylated P38. Control+NC: HUVECs in normal glucose level with negative control; Control+miR-28 mimics: HUVECs in normal glucose level with miR-28-3p mimics (1uM for 48 hours); HG+NC: HUVECs under high glucose for 48 hours with negative control; HG+miR-28 inhibitor, HUVECs under high glucose for 48 hours with miR-28-3p inhibitors for 48 hours. *P < 0.05, **P < 0.01, ***P < 0.001.

3A

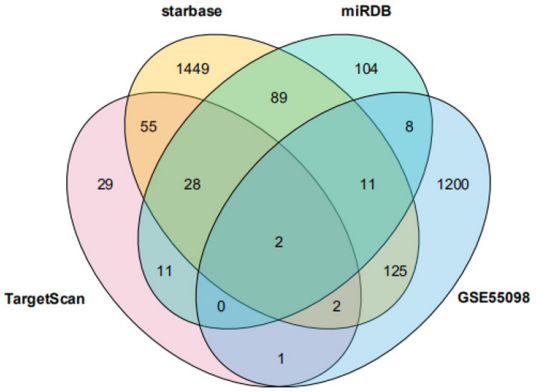

3C

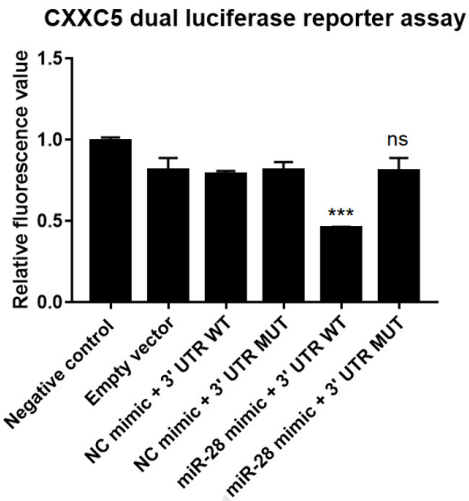

3B

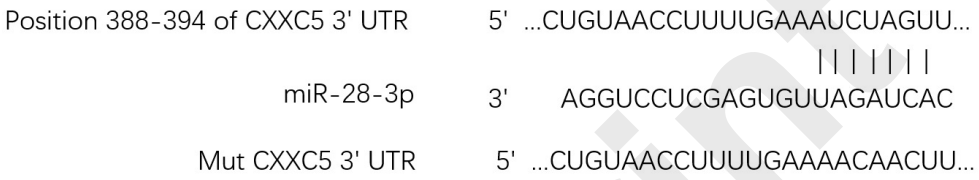

CXXC5 is a direct target gene of miR-28-3p. Fig 3A: We used Targetscan, Starbase, and miRDB to predict the possible gene target of miR-28-3p in GSE55098, a dataset consisting of proteins from newly diagnosed type 1 diabetic patients. Only two proteins, namely CXXC5 and PARP8, poly(ADP-Ribose) polymerase family member 8, were found to be the potential target. There was no observed correlation between the expression levels of PARP8 and miR-28-3p in high-glucose cultured HUVEC. Therefore, the subsequent investigations were centered on miR-28-3p and CXXC5. Fig. 3B, prediction of miR-28-3p binding sites in the 3'-UTR of the CXXC5 gene, along with the mutated 3' UTR for dual luciferase reporter assay. Fig. 3C, dual luciferase reporter assay. Transfection with the miR-28-3p mimic significantly decreased the relative luciferase activity of the CXXC5-WT 3'-UTR compared with that in cells following the transfection of mimic NC. The effect was abolished when the nucleotides in the seed binding site of the CXXC5 3'-UTR were mutated. *P < 0.05, **P < 0.01, ***P < 0.001.

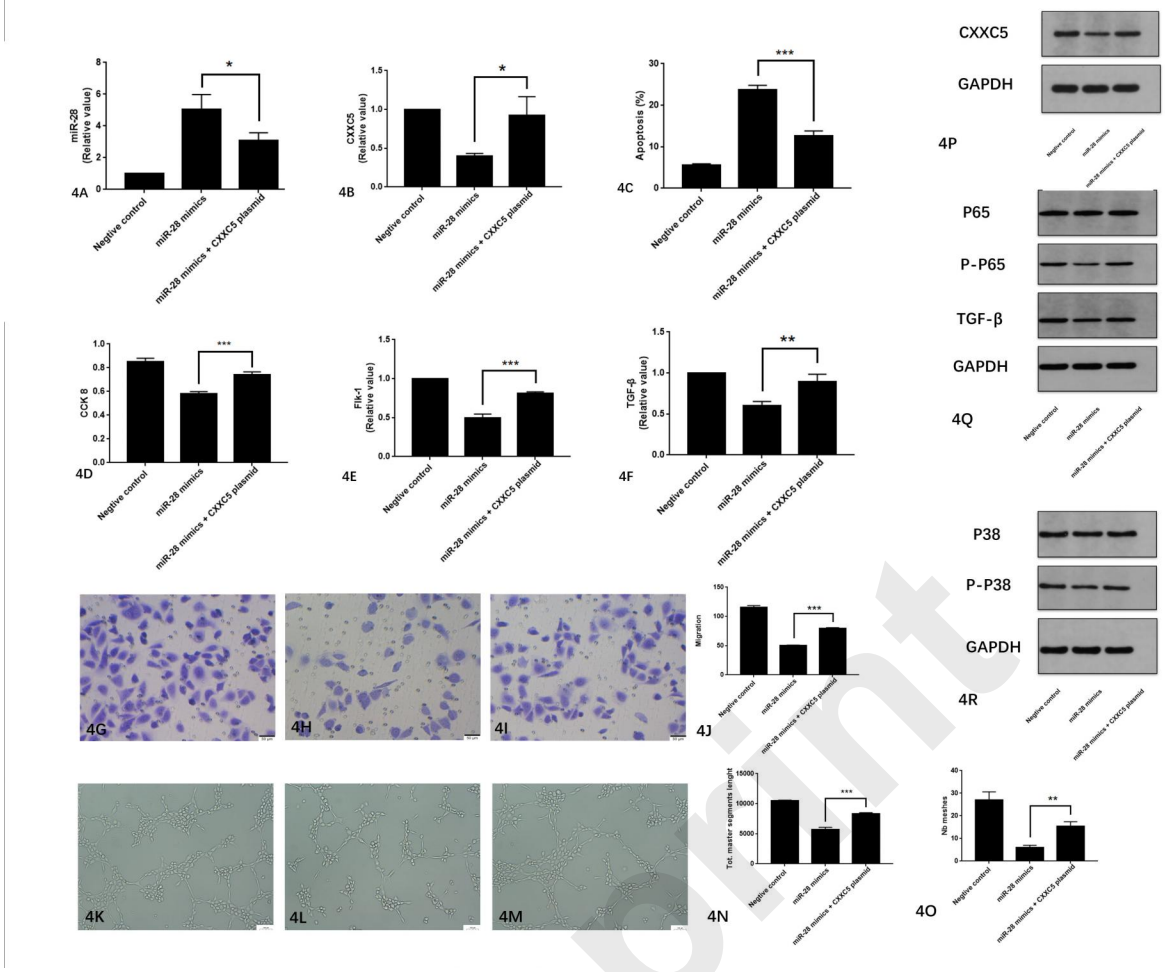

Molecular expression and HUVECs function under miR□28-3p mimics and CXXC5 overexpression. 4A, 4B, 4E, 4F: PCR results; C: Apoptosis detected by flow cytometry; 4D. Cell proliferation assessed by CCK8. 4A, 4B, 4E, 4F: PCR results; 4C: Apoptosis detected by flow cytometry; 4D. Cell proliferation assessed by CCK8. Fig 4G-4J: Cell migration detected by Transwell assays. Cell migration detected by Transwell assays. Fig. 4G: Negative control; Fig. 4H: miR-28 mimics; Fig. 4I: miR-28 mimics+CXXC5 plasmid. Fig. 4G to I: one representative picture of vessel formation assay. Fig. 4J: quantitative analysis of Transwell assays. Fig 4K-4O: Vessel formation assay. Fig. 4K: Negative control; Fig. 4L: miR-28 mimics; Fig. 4M: miR-28 mimics+CXXC5 plasmid. Fig. 4K to 4M: one representative picture of vessel formation assay. Fig. 4N & 4O: quantitative analysis of vessel formation. Fig 4P-4R: Western blot results on co-overexpression of both miR-28-3p and CXXC5. GAPDH is the internal reference. P-P65: Phosphorylated P65; P-P38: Phosphorylated P38. Negative control: HUVECs in normal glucose level with negative control; miR-28 mimics: HUVECs in normal glucose level with miR-28-3p mimics (1uM for 48 hours); miR-28 mimics+CXXC5 plasmid: HUVECs in normal glucose level with miR-28-3p mimics and CXXC5 overexpression plasmid. *P < 0.05, **P < 0.01, ***P < 0.001.

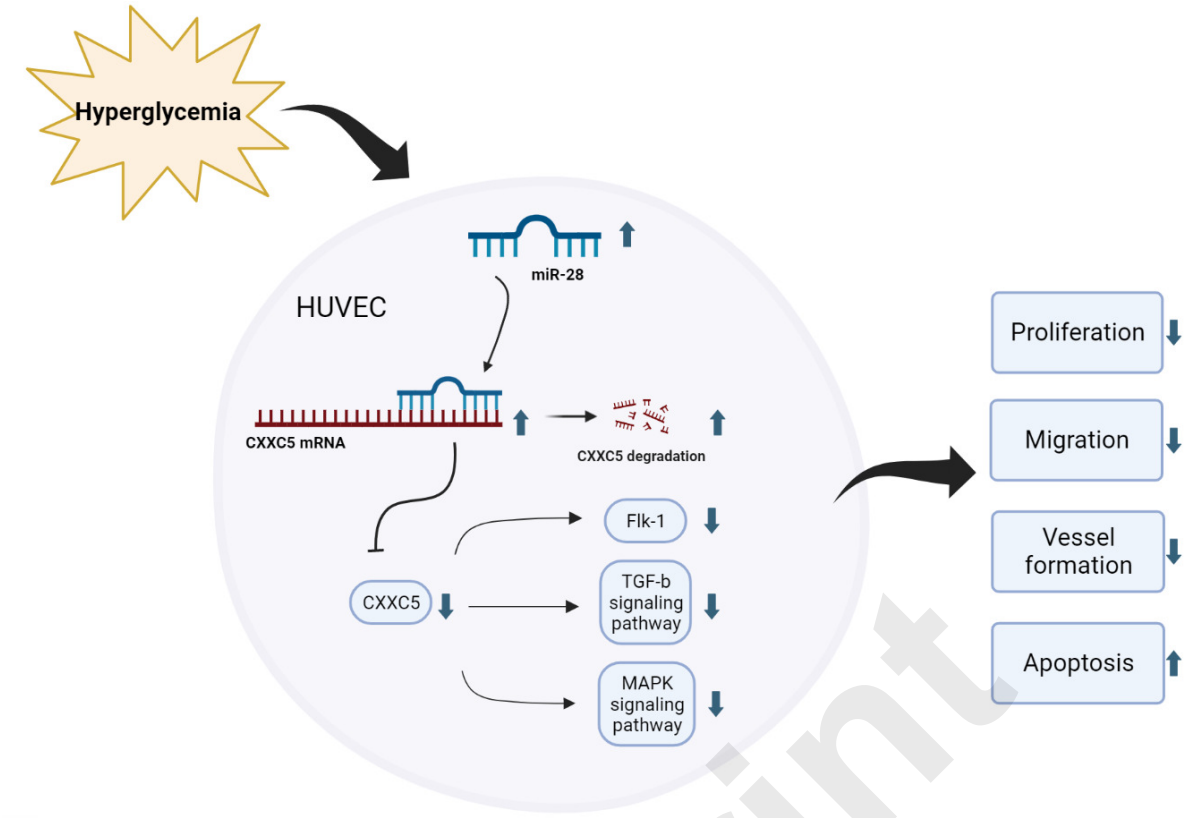

Diagram of the role of miR-28 in high glucose-cultured HUVEC

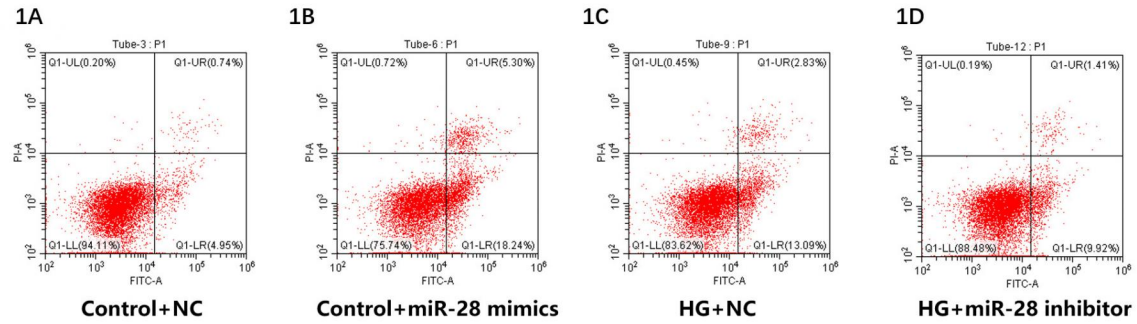

Typical flow cytometry results in apoptosis of Fig 2C. Control+NC: HUVECs in normal glucose level with negative control; Control+miR-28 mimics: HUVECs in normal glucose level with miR-28-3p mimics; HG+NC: HUVECs under high glucose for 48 hours with negative control; HG+miR-28 inhibitor, HUVECs under high glucose for 48 hours with miR-28-3p inhibitors for 48 hours.

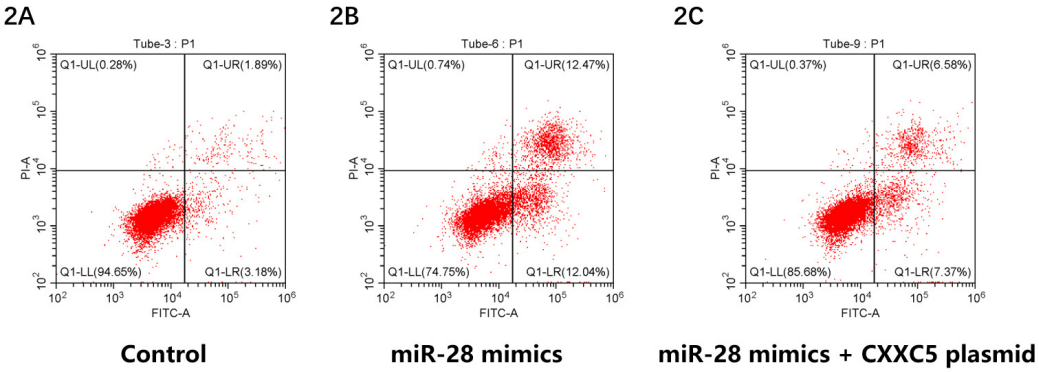

Typical flow cytometry results in apoptosis of Fig 4C. Control: HUVECs in normal glucose level with negative control; miR-28 mimics: HUVECs in normal glucose level with miR-28-3p mimics (1uM for 48 hours); miR-28 mimics+CXXC5 plasmid: HUVECs in normal glucose level with miR-28-3p mimics and CXXC5 overexpression plasmid.